



# A new parallel deep learning algorithm for breast cancer classification

Ahmad Kazemi<sup>a</sup>, Mohammad Ebrahim Shiri<sup>b,\*</sup>, Amir Sheikahmadi<sup>a</sup>, Mohamad Khodamoradi<sup>c</sup>

<sup>a</sup> Department of Computer Engineering, Sanandaj Branch, Islamic Azad University, Sanandaj, Iran.

<sup>b</sup> Computer Science Department, Amirkabir University of Technology, Tehran, Iran.

<sup>c</sup> Department of Mathematics, Izeh Branch, Islamic Azad University, Izeh, Iran.

(Communicated by Madjid Eshaghi Gordji)

---

## Abstract

Now diagnostic methods with the help of machine learning have been able to help doctors in this field. One of the most important of these methods is deep learning, which has gotten good answers in images containing cancer. Increasing the accuracy of deep neural network classifiers can increase the diagnosis of breast cancer. In this paper, we have tried to achieve higher accuracy than non-parallel models with the help of a parallel model of a deep neural network. The proposed method is a parallel hybrid method combining AlexNet and VGGNet networks applied in parallel to mammographic images. The database used in this article is INBreast. The results obtained from this method show a 4% increase compared to some other classification models so that in the type of density 1, it has achieved about 99.7%. In the case of other densities, an accuracy of nearly 99% has been obtained.

*Keywords:* Medical Image, Magnetic Resonance Imaging, parallel convolutional neural network.

---

## 1. Introduction

Breast cancer [31] is the most common cancer that women get. One million new cases of the disease are diagnosed each year. Unfortunately, despite significant advances in treatment, about 25% of breast cancer patients die each year due to the disease. The prevalence and mortality rate of breast cancer varies in different races and geographical locations, and different mechanisms are involved in its onset and progression. Breast cancer is caused by the abnormal growth of abnormal cells in the

---

\*Corresponding author

*Email addresses:* [ahmadkazemi\\_2006@ymail.com](mailto:ahmadkazemi_2006@ymail.com) (Ahmad Kazemi), [shiri@aut.ac.ir](mailto:shiri@aut.ac.ir) (Mohammad Ebrahim Shiri), [sheikahmadi@eng.ui.ac.ir](mailto:sheikahmadi@eng.ui.ac.ir) (Amir Sheikahmadi), [mohammad\\_moradi57@yahoo.com](mailto:mohammad_moradi57@yahoo.com) (Mohamad Khodamoradi)

breast [32]. In both benign and malignant tumors, there is rapid and abundant cell growth. The process of cell proliferation in benign tumors stops at a certain stage; in malignant tumors, this growth continues uncontrollably to the extent that, if left untreated, it affects all parts of the body.

The most common type of breast cancer is cancer of the mammary duct, and because it is more common in the upper and outer quarters of the breast, about half of all breast cancers are found in the upper and outer quarters [32, 37].

Sometimes, a diagnosis of breast cancer is made after the signs and symptoms appear. In some cases, people with breast cancer have no symptoms. So doctors often use a series of additional tests to diagnose breast cancer. If the doctor finds signs of breast cancer on a mammogram or has symptoms that could mean breast cancer, he or she will get more tests to make sure the cancer is present or not [26].

There are several ways in which a doctor can examine breast tissue and judge possible masses. Fine Needle Aspiration (FNA) testing is a low-cost, easy, fast, high-precision, the almost no-side method that can be performed on an outpatient basis. In the FNA method, fluid extracted from breast tissue is tested for cytological properties. After extracting the patient's cytological characteristics, it should be possible to determine whether the mass is benign or malignant. In cases where it is impossible to determine whether the disease is benign or malignant, the use of computer algorithms and machine learning techniques is a good guide for the physician. These methods, along with methods of obtaining information, have been able to replace laboratory methods. The most commonly used methods are mammography, ultrasound, MRI, and biopsy. Mammography uses X-rays to take pictures of buildings inside the breast. This is a quick and simple method and has facilitated the diagnosis and improved patients' treatment results due to early diagnosis of the disease [36].

In healthy women, screening mammography is used as an early diagnostic method. In this way, a basic mammogram is performed between the ages of 35 and 39, and then from the age of 40 onwards, mammograms are performed annually so that if there is a cancerous mass in the breast in the early stages, it can be detected [36, 27].

In recent years, interest in research into intelligent algorithms in the diagnosis and classification of diseases, especially cancer, has increased sharply. One of the important tasks of medical diagnosis is to classify tumors. Software computational methods are very important in diagnosing medical diseases due to their classification function. Deep learning [39] is becoming a way to analyze medical images and aims to learn high-level data summaries using hierarchical architecture and is an emerging approach that is widely used in artificial intelligence. Deep learning is one of the sub-disciplines of machine learning that aims to learn high-level abstracts of data using hierarchical architectures and is an emerging approach widely used in artificial intelligence.

The most important advantage of using convolutional neural networks (CNN) is its ability to automatically extract [12] image properties using deep learning concepts [31, 32]. Due to this very important advantage in recent years, the use of CNN's to diagnose diseases in various medical applications has been considered by researchers. For example, in the diagnosis of diabetic retinopathy (DR) or ocular diabetes, which due to diabetes in this group of patients, the retinal vessels are deformed and widened for better blood supply, from CNN networks, to extract features Retinal images were obtained and then the retinal blood vessels were segmented by group learning [37, 26]. CNN's are also used to diagnose the progression of various diseases [36, 27]. Also, in another study, a comparison between two CNN structures with the dimensions and number of multiple layers was performed to diagnose the disease as accurately as possible [39]. Other applications of CNNs in the diagnosis and classification include the correct diagnosis of polyps [34] during colonoscopy [24], the automatic detection of pulmonary embolism in CT scan images [2], and diagnostic assistance. Breast cancer cell division computer in pathology databases [3], detection of lymph nodes in CT images and diagnosis

of abdominal lymph nodes [22], classification of pulmonary diseases [19], and automatic diagnosis of anatomy in CT images [6] The applications of CNNs are not limited to the subject of diagnostic systems. Still, they have also performed well in measuring and segmenting medical images. Some of these applications include pancreas segmentation on tomographic scan [1], segmentation of pediatric brain images [9], neural membrane segmentation on electron microscopic images [33], segmentation of knee cartilage images on MRI scan [10], and layer thickness measurement [21] and dozens of other fields.

## 2. Materials and Methods

Much work has been done for medical diagnosis using traditional methods, which usually involve two steps: feature extraction and data classification. However, in recent years, more scientists have chosen deep learning in pattern recognition due to the ability of the neural network to learn. As a result, they have achieved many research achievements.

[43] A method for identifying masses in mammographic images with dense breast tissue using image processing methods and convolutional neural networks is described. DDSM data are used to identify the suspicious area (asymmetric area), however, a method is needed to reduce the positive error and increase productivity. Convolution neural network for classifying breast tissue density as well as for diagnosis The final mass is applied. In mass classification, the use of CNN is very effective. Even in cases with a simple structure, it is possible to achieve 97% of the masses. It is noteworthy that a limited number of classification sources have preferred density over mass identification. Detection of mass and non-mass areas with density has significant results compared to similar works. The use of convolutional neural networks is an essential step in extracting features.

To solve the DCNN problem, a transfer learning method has been defined [30] and it is shown that it is possible to detect mass in mammographic images using the transfer learning method. A DCNN structure consists of eight weight layers consisting of 5 conduction layers and 3 fully connected layers. First, the tutorial uses 1.2 million normal images to classify 1000 classes. Then, by changing the last continuous layer, 1656 areas have been done for classification of two classes (normal-mass). The diagnostic test on 198 mammographic images includes 99 normal images and 99 mass images. The test results show a sensitivity of 89.9% and a positive error of 19.2%. The results show that DCNN, together with the transfer learning method, has the ability to perform mass recognition by computer.

In [13], the general framework is based on two-dimensional section images. By surface-to-surface analysis of two-dimensional sections of digital tomographic images, the pattern is automatically learned by convolutional neural networks. Then learn to apply multiple slices and the images are categorized based on the extracted features. Using CAD and its expansion, 5040 two-dimensional slices of images from 87 sets are evaluated. Experimental results show that the proposed method offers higher accuracy than other methods, such as the Boltzmann method.

In [11], the segmentation step is performed based on the extracted edges of the tumor border. But due to some damaged and indeterminate edges, it is difficult to identify. Area-based segmentation increases the accuracy of classification, and this is because the tumor area is usually brighter than the tissues around the tumor and has an almost uniform density.

In [17], tumor segmentation has been performed on the tumor with regional segmentation techniques. The uniform algorithm is used for automatic segmentation of tumor candidate areas and overall, the recovery rate is 90% for tumor masses. But the criterion used for analysis is only based on the location of the tumor and not on the quality of the segmentation.

In [25] they presented a tumor detection system for the correct classification of breast masses into normal, abnormal, benign or malignant categories. The proposed method examines two datasets: MIAS and DDSM. A new algorithm has been used to classify based on the combination of top-hat conversion and gray surface interaction matrix with reverse diffusion neural network. The final accuracy obtained is reported to be 62.97% on average.

### 3. Convolution neural network

Convolution neural networks are a model of multilayer neural networks and, like other neural networks, are composed of weighted and biased neural layers with the ability to learn. These networks are designed to work well for matrix-structured inputs (two-dimensional and three-dimensional). The neural network typically consists of convolutional, pulling, and fully connected layers [14].

- **Input Layer:** The first layer of each CNN used is the ‘input layer,’ which takes images, resizes them for passing onto further layers for feature extraction.
- **Convolution Layer:** The next few layers are ‘Convolution layers,’ which act as filters for images, finding out features from images and calculating the match feature points during testing.
- **Pooling Layer:** The extracted feature sets are then passed to the ‘pooling layer.’ This layer takes large images and shrinks them down while preserving the most important information in them. It keeps the maximum value from each window it preserves the best fits of each feature within the window.
- **Rectified Linear Unit Layer:** The corrected linear unit replaces the negative numbers of the addition layer with 0.
- **Fully Connected Layer:** The final layer is the fully connected layers which take the high-level filtered images and translate them into categories with labels.

In a multilayer neural network, the neural network receives the input and sends it to several hidden layers. Each hidden layer comprises several neurons in the form of a vector, each of which is completely connected to all the neurons in its previous layer. The neurons in each layer act independently and do not share communications and weights. The last layer of this network is the output layer, which is ultimately responsible for determining the data class.

The layers of this network, unlike multilayer neural networks, consisting of neurons in three dimensions. In some articles, they are also called tensors. The first level is the convolution layer, which can extract new features from the image using various kernels. This is followed by Max pooling, which reduces the size and number of network parameters. The output of this layer is sent to the complete connection network layer after being converted to a one-dimensional vector. conventional neural network algorithms are used in this layer. The convolution + max-pooling block, known as the convolution layer, can be repeated many times to build a deeper network. The user also determines the number of Fully connected layers. Convolutional neural networks have shown their efficiency in image processing applications such as image classification, object recognition, and image content retrieval. Good results have been achieved in solving the problem of image classification [23]. High accuracy has been achieved in the issue of object recognition [5]. In content retrieval of images, it has achieved good performance compared to classical methods such as color, shape, and texture [16].

The sheer number of parameters that can be learned on CNN is one of its challenges. Today, its computational implementation on the GPU by in-game text frameworks such as Tensorflow and

CNTK, which support the development of powerful mouthpieces, has enabled the widespread use of CNN, making it a practical tool in image and video processing studies. Figure 1 shows the difference between a convulsive neural network and a normal neural network. As shown in the figure, all the neurons are connected in a multilayered neural network, but the neurons are located in three dimensions in a CNN. In Figure 1-b, the input layer marked in purple can be an input image to the grid that has length, width, and depth and represents three purple, yellow, and blue channels in the image.

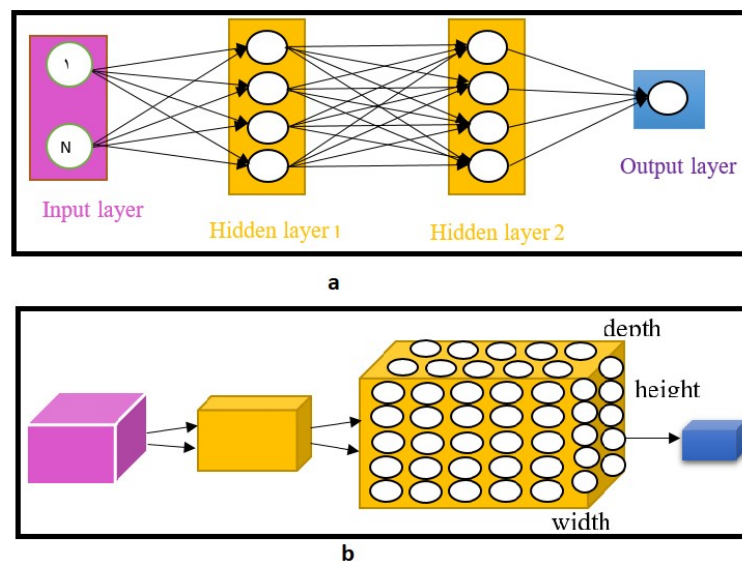


Figure 1: a) normal neural network, b) convolutional neural network

In less than a decade, artificial convolutional neural networks have played an important role in deep learning by developing computer processing power in vital applications such as medical image processing and car systems with increasing success. Have been together. The use of convolutional networks such as Google Net, and AlexNet, due to the use of deeper layers compared to conventional neural networks, can significantly differ in the processing of medical images and the screening of diseases.

The AlexNet network was introduced at the 26th Conference on Neural Information Processing Systems in 2012 [18]. AlexNet looks like a simple architecture with intricate layers stacked on top of each other and perfectly connected to the top layers. What makes this model different is the speed of the task and a "GPU" for learning. In the 1980s, CPUs were used to learn a neural network, but AlexNet used GPUs to increase learning speed tenfold. Various have been collected. AlexNet consists of 5 convolutional layers, three pooling layers, and two fully connected layers and has about 60 million free parameters for training.

AlexNet is a deep convolutional neural network architecture, which sums up to a total of 22 layers. The convolution layer, the main building block in the network, constitutes the first layer and is followed by a RELU transfer function. Next is a max pool, which dynamically lessens the image size. This limits the measure of system calculation, parameters, and shields from overfitting. The next three layers follow a similar pattern (CONV-RELU-POOL). Layers 7, 8, 9, 10, 11, 12 follow the pattern of convolution followed by a transfer function (CONV-RELU). The thirteenth layer is max-pooling. After which, the network is composed of few fully connected layers. Next is a simple linear layer, which is followed by dropout and threshold layers. Finally, a 4- way softmax classifier is managed to order the images into different classes [35].

#### 4. Proposed method

This study aimed to present a model of deep parallel networks to differentiate between images related to breast cancer. Accordingly, the proposed method has steps that we will discuss in the following.

In general, a convolutional neural network is a hierarchical neural network in which the convolutional layers are interspersed with the pooling layers [4], followed by several fully connected layers. In these layers, the CNN network uses different kernels to convolve the input image and the middle feature maps, thus creating different feature maps. One of the interesting methods of managing the convolutional layers is the Network in Network (NIN) method, in which the main idea is to replace the convolutional layer with a small perceptron neural network that performs the separation operation with the help of Equation (4.1) and includes several fully connected layers. The activation functions of this network are nonlinear, and nonlinear neural networks replace linear filters [20]. This method achieves good results in categorizing images.

$$y = f \left( \sum_i w_i x_i \right) \quad (4.1)$$

A pooling layer is usually placed after a convolutional layer and can reduce the size of feature maps and network parameters. Like convolutional layers, pooling layers are resistant to displacement due to the consideration of neighboring pixels in their calculations. Pooling layer implementations using the max (max-pooling [20]) function (Figure 2 and Equation (4.2)) and the Average (Average pooling [20]) function are the most common implementations. Using a max-pooling filter with a size of  $2 \times 2$  and a feature map with a size of  $8 \times 8$  will create an output with a  $4 \times 4$ .

$$MP_{i,j} = \max(I_{i,j} C_{i,j}) \quad (4.2)$$

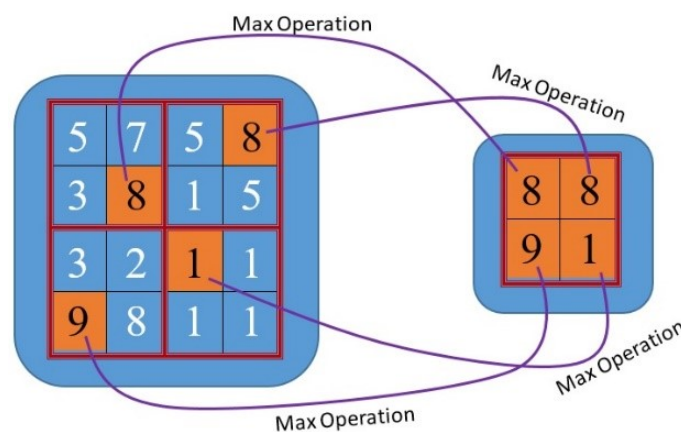


Figure 2: Example of Max Pooling

##### 4.1. Network structure

With recent advances in the use of CNN in computer vision, popular models of convolutional neural networks have emerged. The method introduced (Figure 3) is a parallel deep learning model for classifying and ultimately diagnosing cancerous tumors. AlexNet and VGGNet [44] are two architectures for convolutional neural networks that have been considered in this parallel model.

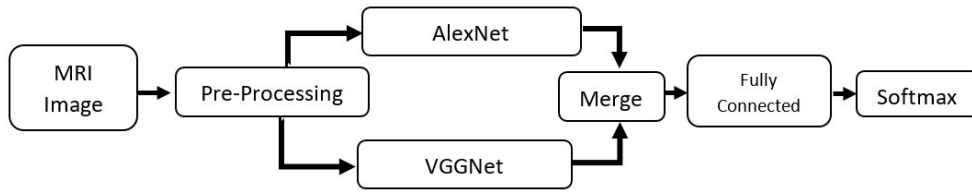


Figure 3: Proposed parallel neural network

General AlexNet consists of 5 layers of convolution and three fully connected layers. This architecture receives  $128 * 128$  images as input and then processes the input image by performing sequential convolution and pooling operations and finally sending the results to the fully connected layers. The second framework presented in this research is a VGGNet based CADx framework that can be done in two steps: feature selection and classification. In the following, the details of this model with input size  $256 * 256$  are provided (Figure 4).

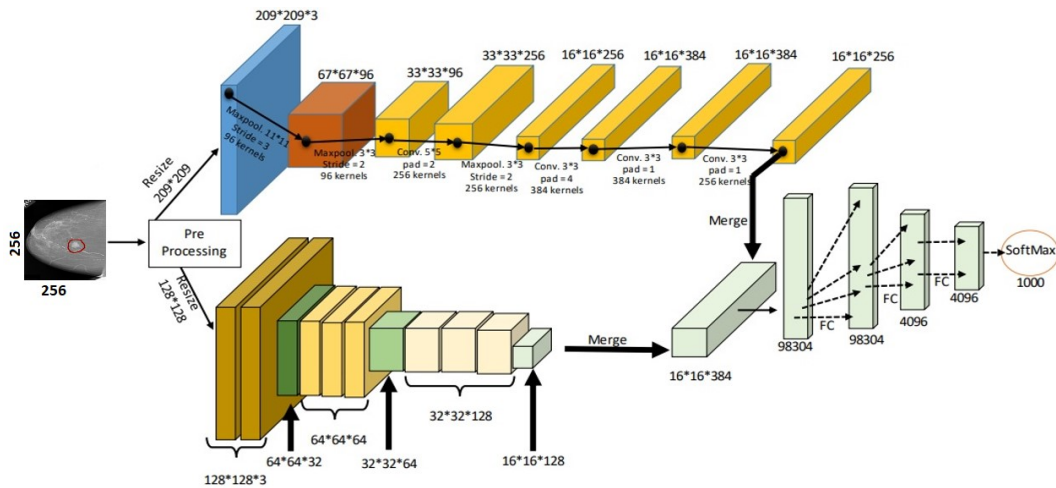


Figure 4: The final model of a parallel deep neural network

The proposed method consists of two frameworks: Medical image pre-processing and Dual-CNN model design. It is used to simplify the morphological operation for preprocessing images [28].

Because two different networks are used in this parallel model, the size of their input images is also different. The optional AlexNet network input is  $209 * 209$ , and the optional VGGNet network input [40] is  $128 * 128$ .

After the preprocessing operation, two layers of the created neural network should be applied to the data. Each layer is a 3D array of size  $s1 * s2 * f$  (width, height, and depth) in this network. In each layer,  $f$  represents the channel depth,  $s1$  and  $s2$  represent the spatial dimensions of the data. The input layer also specifies the amount of red, green, or blue parameters of the image. The structure of the AlexNet network contains 8 layers of convolution and ReLU. These layers are followed by 8 additional computational layers, which alternate between convolution and ReLU. Finally, the resulting matrix is combined with the VGGNet network matrix to create a matrix with  $16 * 16 * 384$ . The computational process of this network is presented in Table 1.

Table 1: Architectural details of the modified AlexNet model.

Layer No.	Layers	Kernel size(s1*s2)	number of Kernels	Output shape
1	Input Image	-	-	3*256*256
2	Image Resize	-	-	3*209*209
3	Max Pooling 1	(11*11)	96	67*67
4	Max Pooling 2	(3*3)	96	33*33
5	Convolution 1+ Rectifier Unit	(5*5)	256	33*33
6	Max Pooling 3	(3*3)	256	16*16
7	Convolution 2+ Rectifier Unit	(3*3)	384	16*16
8	Convolution 3+ Rectifier Unit	(3*3)	384	16*16
9	Convolution 4+ Rectifier Unit	(3*3)	256	16*16

The structure of the VGGNet network contains 8 layers. This network consists of 13 circular layers, each of which is equipped with more filters. After each of these layers is a ReLU layer, these layers are followed by 8 additional computational layers, which alternate between the fully connected part and the ReLU. The computational process of this network is presented in Table 2.

Table 2: Architectural details of the modified AlexNet model.

Layer No.	Layers	Kernel size(s1*s2)	Output shape
1	Input Image	-	3*256*256
2	Image Resize	-	3*128*128
3	Convolution 1+ Rectifier Unit	(3*3)	32*128*128
4	Convolution 2+ Rectifier Unit	(3*3)	32*128*128
5	Max Pooling 1	(2*2)	32*64*64
6	Convolution 3+ Rectifier Unit	(3*3)	64*64*64
7	Convolution 4+ Rectifier Unit	(3*3)	64*64*64
8	Convolution 5+ Rectifier Unit	(3*3)	64*64*64
9	Max Pooling 2	(2*2)	64*32*32
10	Convolution 6+ Rectifier Unit,	(3*3)	128*32*32
11	Convolution 7+ Rectifier Unit,	(3*3)	128*32*32
12	Convolution 8+ Rectifier Unit,	(3*3)	128*32*32
13	Max Pooling 3	(2*2)	128*16*16

In the VGGNet network, a set of images is inserted into the first convolution operation and used in the next layer as Equation (4.3):

$$C_{ij} = \sum \sum (H_{m,n} * I_{i+m,j+n}) + b \quad (4.3)$$

After the operation related to the combination of features, the Fully Connected operation is performed three times, then in the stage of collecting the results and the final classification, a Softmax operation is performed (Equation (4.4)) and as a result, the most probabilities will be considered.

$$P_{class} = arg \max(s) \quad (4.4)$$

Here P is the class label of the presence or absence of the tumor and S is the predicted probability of the model implemented in the final stage of the proposed system.

#### 4.2. Network training

Both network models use the same method for training, which is a basic method in convolutional neural networks. The training method in each convolution neural network consists of two steps: Feedforward and backpropagation. In the first step, the input image enters the network with the help of Point multiplication and convolution. The point multiplication is done between the input and the parameters of each neuron, and then the network’s output is calculated. Here, to set the network parameters, the output result is used to calculate the network error. To do this, using an error function, the network output is compared with the correct answer, and the error rate is obtained.

Forward Propagation (FP) is a process in which the previous layer’s output is considered the input of the current layer. To avoid error, the neurons in each layer must operate with a nonlinear activation function. Since the first layer only receives pixel values, it has no activation function. From the second layer to the last layer, nonlinear activation functions are used. Therefore, the output of each layer can be expressed as follows:

$$Z^l = w^l * x^l + b^l \tag{4.5}$$

Here  $l$  represents the  $l$ th layer, and  $*$  is the convolution action.  $W$ ,  $b$ , and  $x$  are the weight matrices, the bias matrix, and the input weights of the next layer, respectively. The activation function is nonlinear. If  $l = 2$  then  $x^{2-1} = x^1$  is an image matrix whose elements are pixel values. If  $l > 2$ ,  $x^{l-1}$  is a feature maps matrix  $a^{l-1}$  that is extracted from layer  $(l-1)$ . As a result,  $a^L$  represents the final output vector.

Backward Propagation is a supervised learning method. It first selects the cost function based on the output and target values, calculates the error vectors, and updates the  $w_l$  and  $b_l$  parameters. This operation is performed in two steps as follows:

The first step involves selecting the cost function.

A cost function must meet two characteristics:

1. Must be able to calculate the average.
2. In addition to the output values, it should not depend on any neural network activation values.

The function that can be used here instead of the softmax function is Cross-Entropy ( $E_0^L$ ) function. This function is used to classify a single class (Equation (4.6)). In other words, an example can only belong to one class. We will examine both models.

$$E_0^L = -\frac{1}{1} \sum_{i=1}^n \sum_{k=1}^N \left[ t_k^L \ln a_k^L + (1 - t_k^L) \ln(1 - a_k^L) \right] \tag{4.6}$$

The  $n$  is the total number of training sets.  $t_k^L$  is the target value for the  $k$ th output layer and  $a_k^L$  is the actual output value of the output layer.

### 5. Experimental setup

#### 5.1. Dataset

In the proposed image classification method, the appropriate data set will first be selected, and then the tagging operation will be performed. The images are then converted to a feature vector. A feature selection method identifies the useless features and selects a limited number of more important features. This can increase the final accuracy of the classification.

Mammographic images from the INbreast database were originally collected from the Centro Hospitalar de S. Joao [CHSJ], Breast Center, Porto. The INbreast database collects data from August 2008 to July 2010, including 115 items with 410 images [31]. Of these, 90 were women with the disease in both breasts. Four different breast diseases are listed in the database, including Mass, Calcification, Asymmetry, and Distortions. The images in this database have two perspectives: Craniocaudal (CC) and medial oblique (MLO), and breast density is divided into four categories according to BI-RADS standards [32], completely fat (density 1), dense (density 2), Dense heterogeneous (density 3) and very dense (density 4) [15].

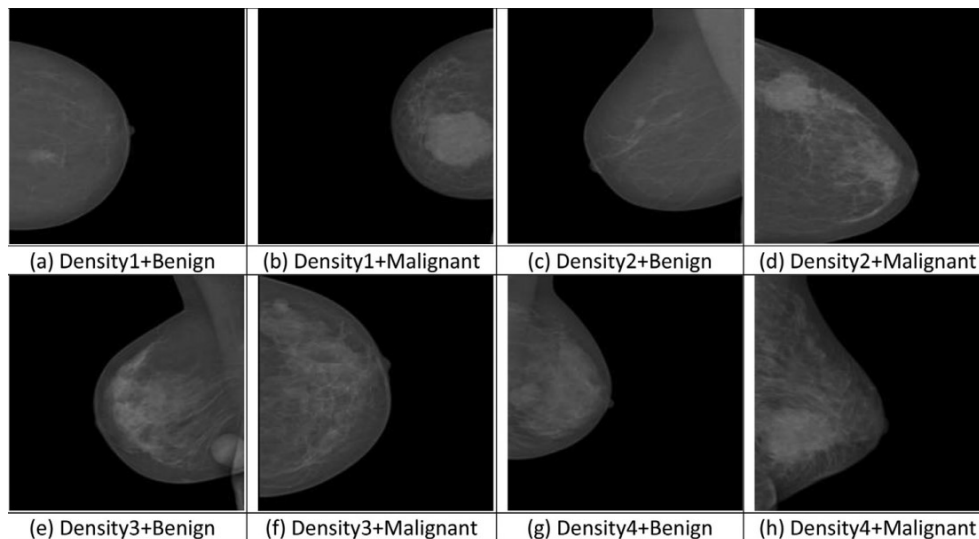


Figure 5: INBreast dataset

The second PLCO dataset is a comprehensive dataset for the analysis of breast cancer incidence and mortality. However, this file only contains information about the first breast cancer diagnosed in the trial. This dataset contains a record for approximately 78,000 women.

### 5.2. System implementation and training

Learning is one of the most important steps in categorizing images. In this study, the aim is to use deep learning to increase the performance of the learning algorithm evaluator function and continue to reach the desired state, and also to classify without user intervention and automatically by the model produced from the above steps. Finally, the model produced is expected to work well on the test data.

Both system models were performed using MATLAB software on a workstation with an Intel Xeon Silver CPU with 32 GB of RAM and an NVIDIA Quadro P4000 GPU with 8 GB of memory. All RGB images have been resized to 256\*256 and all pixel values in the range [0, 1] have been normalized to make the system computationally efficient.

For better experiments, 75% of the set is used as training data and 25% of the set is selected for testing. The Adam optimizer [42] with an initial learning rate of 0.001 has been used to train networks, resulting in a gradual decrease in learning by a factor of 0.1 until learning stagnates.

### 5.3. Evaluation metrics

The classification of medical images is done by testing the model produced with different criteria to produce a reliable method ultimately. A threshold is set for the criteria to reach the optimal value in case of the poor performance of the classification parameters in the search space. To ensure

the correct operation of the proposed model, we try to apply the theory of the proposed method to various algorithms so that we can have a stronger evaluation and comparison of the work done compared to traditional and manual methods. Ultimately, the goal is to achieve an efficient and reliable model by increasing the correct classification accuracy.

The most important evaluation criteria in image classification are precision, sensitivity(Recall), specificity, accuracy, F-criterion, and classification error, which are shown in the following relations, respectively.

The accuracy of the classification will indicate the strength of the proposed method in classification. This accuracy will be calculated using Equation (5.1).

$$\text{Accuracy} = \frac{TP + TN}{TP + FP + FN + TN} \quad (5.1)$$

Sensitivity represents how good a test is at detecting the positives (i.e., true positive rate) and calculated by using Equation (5.2).

$$\text{Sensitivity(Recall)} = \frac{TP}{TP + FN} \quad (5.2)$$

Specificity represents how many good a test is at avoiding incorrect answers. This can be calculated using Equation (5.3) (i.e., real negative rate).

$$\text{Specificity} = \frac{TN}{TN + FP} \quad (5.3)$$

Precision represents a positive predictive value and has been calculated using Equation (5.4).

$$\text{Precision} = \frac{TP}{TP + FP} \quad (5.4)$$

In all these formulas; TP = true positive, TN = true negative, FP = false positive and FN = false negative.

## 6. Results

At this point, after modeling, the results of modeling should be evaluated. The evaluation results improve the model and make the model usable. To check the accuracy of the model, it is first necessary to divide the available data into three sections: training, testing, and validation. The data of the training section produces the model and the data of the experimental section, with the help of a number of records, tests the produced model and determines the label related to the mentioned records.

The data set used for the first phase of our system includes a data set with 3000 images in 4 mentioned modes, which has been trained on 2000 images and tested on 1000 images. The proposed model is classified as binary with the help of various performance criteria (accuracy, sensitivity, specificity, etc.) and softmax performance introduced in the previous section, the results of which are presented in Table 3. An accuracy of 0.991 for the low-density mode indicates that the proposed model for the first phase of the proposed system can provide promising results.

Table 3: Performance evaluation of softmax classifier in INBreast dataset

METRICS	INBREAST DATASET			
	Density 1	Density 2	Density 3	Density 4
F1	0.9890	0.9887	0.9889	0.9888
ACCURACY	0.9917	0.9899	0.9801	0.9799
SENSITIVITY	0.9910	0.9910	0.9902	0.9902
PRECISION	0.9921	0.9913	0.9909	0.9902
SPECIFICITY	0.9923	0.9916	0.9914	0.9914

The data set used for the second phase of our system includes PLCO data set with 5120 images in 4 mentioned modes, which has been trained on 3700 images and tested on 1420 images. The proposed model is classified as binary with the help of various performance criteria (accuracy, sensitivity, specificity, etc.) and softmax performance introduced in the previous section, the results of which are presented in Table 4. An accuracy of 0.987 for the low-density mode indicates that the proposed model for the first phase of the proposed system can provide promising results.

Table 4: Performance evaluation of softmax classifier in INBreast dataset

METRICS	PLCO DATASET			
	Density 1	Density 2	Density 3	Density 4
F1	0.9812	0.9803	0.9799	0.9791
ACCURACY	0.9871	0.9871	0.9870	0.9870
SENSITIVITY	0.9892	0.9892	0.9889	0.9887
PRECISION	0.9903	0.9898	0.9898	0.9897
SPECIFICITY	0.9903	0.9903	0.9903	0.9901

The results of both Tables 3 and 4 show the suitability of the proposed system in 4 possible cases for breast cancer. Now it is possible to compare the performance of the proposed method with other possible methods and gain more confidence in its performance.

## 7. Discussion

This section (Table 5.) compares two deep classification models, two parallel deep models, a support vector machine method, and a multilayer general neural network with the proposed model in terms of evaluation criteria and 4 breast cancer cases.

Table 5: Compare with different models in INBreast dataset

Methods/Metric		Density 1	Density 2	Density 3	Density 4
AlexNet	Accuracy	0.9402	0.9402	0.9311	0.9311
	Sensitivity	0.9421	0.9419	0.9314	0.9312
VGGNet	Accuracy	0.9401	0.9401	0.9309	0.9299
	Sensitivity	0.9416	0.9403	0.9323	0.9302
Parallel AlexNet	Accuracy	0.9567	0.9536	0.9398	0.9398
	Sensitivity	0.9595	0.9537	0.9398	0.9417
Parallel VGGNet	Accuracy	0.9553	0.9516	0.9398	0.9216
	Sensitivity	0.9557	0.9519	0.9399	0.9222
SVM	Accuracy	0.9001	0.8700	0.8335	0.8301
	Sensitivity	0.9012	0.8705	0.8357	0.8351
NN	Accuracy	0.8284	0.7925	0.7575	0.7575
	Sensitivity	0.8297	0.7929	0.7593	0.7593
Proposed Method	Accuracy	0.9917	0.9899	0.9801	0.9799
	Sensitivity	0.9910	0.9910	0.9902	0.9902

Table 5 shows that the proposed method performed better than other classification models in all 4 cases of breast cancer. The final step of comparison is to compare with other methods that have been studied on the IN-Breast database. It seems that the proposed method can get a better answer than other studies.

Table 6: Compare with different models in INBreast dataset

Methods/Metric		Density 1	Density 2	Density 3	Density 4	
[38]	2021	Accuracy	97.01	96.87	95.07	94.67
		Sensitivity	97.08	96.87	95.16	94.64
[8]	2018	Accuracy	96.55	96.32	95.95	95.22
		Sensitivity	96.76	96.39	95.96	95.24
[7]	2015	Accuracy	95.00	94.23	90.66	82.00
		Sensitivity	95.00	94.98	90.90	82.00
[41]	2019	Accuracy	88.60	88.12	80.36	80.17
		Sensitivity	88.97	88.15	80.39	80.17
Proposed Method		Accuracy	0.99	0.98	0.98	0.97
		Sensitivity	0.99	0.99	0.99	0.99

According to the comparisons made in Table 6, it is clear that the proposed method has a much better answer in terms of accuracy than the methods presented in [38, 8, 7, 41, 4]. In some cases, the accuracy of the proposed method has been improved by about 4%.

## 8. Conclusions

Breast cancer is one of the most common diseases among women, usually diagnosed by laboratory diagnostic methods. Deep learning methods, especially parallel deep learning, have been used by the medical field for many years. The proposed model includes a combined model of AlexNet and VGGNet, which could be introduced compared to parallel and non-parallel methods, and even compared to the methods presented in some articles and, in some cases, up to 4% improvement.

## References

- [1] R. A. Ali, A. M. Mehdi and R. Rothnagel, *A Rapid 3D z-crossings algorithm to segment electron tomograms and extract organelles and macromolecules*, J. Struct. Biol., 200 (2) (2017) 73-86.
- [2] Sh. Amemiya, H. Takao and Sh. Kato, *Automatic detection of brain metastases on contrast-enhanced CT with deep-learning feature-fused single-shot detectors*, Eur. J. Radiol., 136 (2021) 109577.
- [3] A. Arjmand, S. Meshgini and R. Afrouzian, *Breast Tumor Detection using Convolutional Neural Network in MRI Images*, J. Adv. Signal Process., 3 (2) (2020) 109-117.
- [4] S. Bazrafkan and P. Corcoran, *Semi-parallel deep neural networks (SPDNN), convergence and generalization*, arXiv preprint arXiv:1711.01963 (2017).
- [5] M. Cadoni, A. Lagorio and E. Grosso, *Incremental models based on features persistence for object recognition*, Pattern Recognit. Lett., 122 (2019) 38-44.
- [6] C. Caradu, B. Spampinato and A. Maria, *Fully automatic volume segmentation of infrarenal abdominal aortic aneurysm computed tomography images with deep learning approaches versus physician controlled manual segmentation*, J. Vasc. Surg., 74(1) (2021) 246-256.
- [7] G. Carneiro, J. Nascimento and A.P. Bradley, *Unregistered multiview mammogram analysis with pre-trained deep learning models*, Int. Conf. Med. Image Comput. Comput. Assisted Intervention, Springer, Cham, 2015.
- [8] E. Castro, J.S. Cardoso and J.C. Pereira, *Elastic deformations for data augmentation in breast cancer mass detection*, 2018 IEEE EMBS Int. Conf. Biomed. Health. Inf. (BHI). IEEE, 2018.
- [9] J. Dolz, Ch. Desrosiers, L. Wang, J. Yuan, D. Shen and I. Aved, *Deep CNN ensembles and suggestive annotations for infant brain MRI segmentation*, Comput. Med. Imaging Graphics, 79 (2020) 101660.
- [10] S. Ebrahimkhani and M. Hisham Jaward, *A review on segmentation of knee articular cartilage: from conventional methods towards deep learning*, Artif. Intell. Med., 106 (2020) 101851.
- [11] M.M. Eltoukhy and I. Faye, *An adaptive threshold method for mass detection in mammographic images*, 2013 IEEE Inter. Conf. Signal and Image Processing Appl.. IEEE, 2013.
- [12] V. Fischer, J. Köhler and T. Pfeil, *The streaming rollout of deep networks-towards fully model-parallel execution*, arXiv preprint arXiv:1806.04965 (2018).
- [13] S.V. Fotin, Y. Yin, H. Haldankar, J.W. Hoffmeister and S. Periaswamy, *Detection of soft tissue densities from digital breast tomosynthesis: comparison of conventional and deep learning approaches*, Med. Imaging 2016: Computer-Aided Diagnosis. Vol. 9785. International Society for Optics and Photonics, 2016.
- [14] M.H. Gholizadeh, H. Ghayoumi Zadeh, H. Fatehi Marj and N. Ahmadi Nejad, *The Investigation of Deep Convolutional Neural Network for Diagnosing Breast Cancer in Thermographic Images*, Jundishapur Sci. Med. J., 18 (6) (2020) 615-629.
- [15] G. Hamed, M.A.E.R. Marey, S.E.S. Amin and M.F. Tolba, *Deep learning in breast cancer detection and classification*, Int. Conf. Artif. Intell. Comput. Vision, Springer, Cham, 2020.
- [16] A. Hassan, F. Liu, F. Wang and Y. Wang, *Secure content based image retrieval for mobile users with deep neural networks in the cloud*, J. Syst. Archit., 116 (2021) 102043.
- [17] B. W. Hong and B.S. Sohn, *Segmentation of regions of interest in mammograms in a topographic approach*, IEEE Trans. Inf. Technol. Biomedicine, 14(1) (2009) 129-139.
- [18] A. Karsaz and S. Mohammadian Roshan, *Medical image processing using deep convolutional neural networks*, Electr. Asre Mag., 5 (11) (2019) 23-28.
- [19] T. Liang and Edward Y. Lee, *Interstitial Lung Diseases in Children, Adolescents, and Young Adults: Different from Infants and Older Adults*, Radiologic Clin., 58(3) (2020) 487-502.
- [20] W. Liu, Z. Wang, X. Liu, N. Zeng, Y. Liu and F.E. Alsaadi, *A survey of deep neural network architectures and their applications*, Neurocomputing, 234 (2017) 11-26.
- [21] S. Liuhanen, M. Sallisalmi, V. Pettilä, N. Oksala and J. Tenhunen, *Indirect measurement of the vascular endothelial glycocalyx layer thickness in human submucosal capillaries with a plug-in for ImageJ*, Comput. Methods Programs Biomed., 110(1) (2013) 38-47.
- [22] T. Masuda, T. Nakaura, Y. Funama, K. Sugino, T. Sato, T. Yoshiura, Y. Baba and K. Awai, *Machine learning to identify lymph node metastasis from thyroid cancer in patients undergoing contrast-enhanced CT studies*, Radiography (2021).
- [23] D. Mishkin, N. Sergievskiy and J. Matas, *Systematic evaluation of convolution neural network advances on the imagenet*, Comput. Vision Image Understanding, 161 (2017) 11-19.
- [24] Y. Mori, Sh. Kudo and J. East, *Cost savings in colonoscopy with artificial intelligence-aided polyp diagnosis: an add-on analysis of a clinical trial (with video)*, Gastrointestinal endoscopy, 92 (4) (2020) 905-911.
- [25] B. Mughal, M. Sharif, N. Muhammad and T. Saba, *A novel classification scheme to decline the mortality rate among women due to breast tumor*, Microsc. Res. Tech., 81(2) (2018) 171-180.

- [26] H. Pratt, F. Coenen, D.M. Broadbent, S.P. Harding and Y. Zheng, *Convolutional neural networks for diabetic retinopathy*, Inter. Conf. Med. Imaging Understanding Anal., July 2016.
- [27] Y. M. S. Reddy, R.E. Ravindran and K.H. Kishore, *Diabetic retinopathy through retinal image analysis: A review*, Inter. J. Eng. Technol., 7(1.5) (2018) 19-25.
- [28] M. Salvi, U. Rajendra Acharya, Filippo Molinari and Kristen M. Meiburger, *The impact of pre-and post-image processing techniques on deep learning frameworks: A comprehensive review for digital pathology image analysis*, Comput. Biol. Med., (2020) 104129.
- [29] N. Sharma, V. Jain and A. Mishra, *An analysis of convolutional neural networks for image classification*, Procedia Comput. Sci., 132 (2018) 377-384.
- [30] S. Suzuki, X. Zhang, N. Homma, K. Ichiji, N. Sugita, Y. Kawasumi, T. Ishibashi and M. Yoshizawa, *Mass detection using deep convolutional neural network for mammographic computer-aided diagnosis*, 2016 55th Annu. Conf. Soc. Instrum. Control Eng. Japan (SICE). IEEE, 2016.
- [31] C. Szegedy, W. Liu, Y. Jia, P. Sermanet, S. Reed, D. Anguelov, D. Erhan, V. Vanhoucke and A. Rabinovich, *Going deeper with convolutions*, Proc. IEEE conf. comput. vision and pattern recognition 2015, pp. 1-9.
- [32] C. Szegedy, V. Vanhoucke, S. Ioffe, J. Shlens and Z. Wojna, *Rethinking the inception architecture for computer vision*, Proc. IEEE conf. comput. vision and pattern recognition. 2016.
- [33] E. Takaya, Y. Takeichi, M. Ozaki and S. Kurihara, *Sequential semi-supervised segmentation for serial electron microscopy image with small number of labels*, J. Neurosci. Methods, 351 (2021) 109066.
- [34] M. Taş and B. Yılmaz, *Super resolution convolutional neural network based pre-processing for automatic polyp detection in colonoscopy images*, Comput. Electr. Eng., 90 (2021) 106959.
- [35] A. Unnikrishnan, V. Sowmya and K.P. Soman, *Deep AlexNet with reduced number of trainable parameters for satellite image classification*, Procedia Comput. Sci., 143 (2018) 931-938.
- [36] H.H. Vo and A. Verma, *New deep neural nets for fine-grained diabetic retinopathy recognition on hybrid color space*, IEEE Int. Symp. Multimedia, Dec. 2016.
- [37] S. Wang, Y. Yin, G. Cao, B. Wei, Y. Zheng and G. Yang, *Hierarchical retinal blood vessel segmentation based on feature and ensemble learning*, Neurocomputing, 149 (2015) 708-717.
- [38] J. Wang, Q. Liu, H. Xie, Z. Yang and H. Zhou, *Boosted EfficientNet: Detection of Lymph Node Metastases in Breast Cancer Using Convolutional Neural Networks*, Cancers 2021, 13, 661. (2021).
- [39] J. Wang and R. Yuan, *Automated diagnosis of neonatal encephalopathy on aEEG using deep neural networks*, Neurocomputing, 398 (2020), 95-107.
- [40] J. Wei, Y. Ibrahim, S. Qian, H. Wang, G. Liu and Q. Yu, *Analyzing the impact of soft errors in VGG networks implemented on GPUs*, Microelectron. Reliab., 110 (2020) 113648.
- [41] N. Wu, J. Phang, J. Park, Y. Shen, Z. Huang, M. Zorin and K.J. Geras, *Deep neural networks improve radiologists' performance in breast cancer screening*, IEEE Trans. Med. Imaging, 39 (4) (2019) 1184-1194.
- [42] B. Yin, C. Wang and F. Abza, *New brain tumor classification method based on an improved version of whale optimization algorithm*, Biomed. Signal Process. Control, 56 (2020) 101728.
- [43] M. Yousefi, A. Krzyżak and C.Y. Suen, *Mass detection in digital breast tomosynthesis data using convolutional neural networks and multiple instance learning*, Comput. Biol. Med., 96 (2018) 283-293.
- [44] W. Yu, K. Yang, Y. Bai, T. Xiao, H. Yao and Y. Rui. *Visualizing and comparing AlexNet and VGG using deconvolutional layers*, Proc. 33 rd Inter. Conf. Mach. Learn., 2016.